### Title
A Compartmental Lateral Inhibition System to Generate Contrasting Patterns




### Journal
IEEE Life Sciences Letters, 1(1)

### ISSN
2332-7685



### Authors
Ferreira, Ana Sofia Rufino
Hsia, Justin
Arcak, Murat



### Publication Date
2015-06-01

### DOI
10.1109/lls.2015.2446211

Peer reviewed

HHS Public Access

Author manuscript

*IEEE Life Sci Lett*. Author manuscript; available in PMC 2015 December 07.

Published in final edited form as:

*IEEE Life Sci Lett*. 2015 June ; 1(1): 7–10. doi:10.1109/LLS.2015.2446211.

# A Compartmental Lateral Inhibition System to Generate Contrasting Patterns

**Ana S. Rufino Ferreira**, **Justin Hsia**, and **Murat Arcak**

Ana S. Rufino Ferreira: ana@eecs.berkeley.edu; Justin Hsia: jhsia@eecs.berkeley.edu; Murat Arcak: arcak@eecs.berkeley.edu

## Abstract

We propose a lateral inhibition system and analyze contrasting patterns of gene expression. The system consists of a set of compartments interconnected by channels. Each compartment contains a colony of cells that produce diffusible molecules to be detected by the neighboring colonies. Each cell is equipped with an inhibitory circuit that reduces its production when the detected signal is sufficiently strong. We characterize the parameter range in which steady-state patterns emerge.

## I. Introduction

Lateral inhibition is a mechanism where cell-to-cell signaling induces neighboring cells to diverge into sharply contrasting fates, enabling developmental processes such as segmentation and boundary formation [1]. The best-known example is the Notch pathway in Metazoans where membrane-bound Delta ligands bind to Notch receptors on the neighboring cells. This binding releases the Notch intracellular domain in the neighbors, which then inhibits their Delta production [2], [3], [4]. Lateral inhibition is not limited to complex organisms: a contact-dependent inhibition (CDI) system has been identified in *E. coli* where delivery via membrane-bound proteins causes downregulation of metabolism [5]. Despite the research on these natural pathways, a synthetic lateral inhibition system for pattern formation has not been developed.

We propose a *compartmental* lateral inhibition setup to generate contrasting patterns. This system consists of a set of compartments interconnected by channels as in Figure 1. Each compartment holds a colony of cells that produce diffusible molecules to be detected by the neighboring colonies. Furthermore, each cell has an inhibitory circuit that reacts to the detected signal. To prevent auto-inhibition, the system uses orthogonal diffusible quorum sensing pairs [6], and two types of inhibitory circuits that are able to detect only one type of molecule and produce the other type. In the examples of Figure 1, cells of type *A* produce a diffusible molecule *X* only detectable by cells of type *B*, and cells of type *B* produce a diffusible molecule *Y* only detectable by cells of type *A*.

To derive conditions under which this system will exhibit contrasting patterns, we define a graph where each compartment corresponds to a vertex. The diffusion of molecules between two compartments occurs through the channels and is represented by the graph edges. We

model the diffusion with a compartmental model, and represent the compartment-to-compartment communication by the Laplacian matrix. The edge weights depend on the distance between the compartments and the diffusivity of the quorum sensing molecules. We then use the graph-theoretic notion of *equitable partition* to ascertain the existence of contrasting steady-state patterns. Equitable partitions reduce the steady-state analysis to finding the fixed points of a scalar map. We also show that the slope of the scalar map at each fixed point provides a stability condition for the respective steady-states. Finally, we apply our analysis to an example and study parameter ranges for patterning.

Graph theoretical results have been used to analytically determine patterning by contact inhibition, in networks of identical cells [4]. The present paper employs diffusion for communication between compartments and allows two cell types to avoid auto-inhibition.

Most reaction-diffusion mechanisms rely on one-way communication. A two-way communication mechanism using orthogonal quorum sensing systems has been employed to demonstrate a predator-prey system, [7]. Unlike these results, we implement lateral inhibition between cell colonies within connected compartments, and achieve spatial patterning.

Due to space constraints, all the proofs are provided as supplemental material.

## II. An Analytical Test for Patterning

### A. Composing a Compartmental Lateral Inhibition Model

Consider a network of $N_A$ compartments of type $A$ and $N_B$ compartments of type $B$. Each cell of type $A$ produces diffusible species $X$, and only cells of type $B$ are equipped with a receiver species that binds to $X$ and forms a receiver complex. Similarly, the diffusible species $Y$ is produced by cells of type $B$ and detected by cells of type $A$. We represent the dynamics in each cell type with three modules: the transmitter module where species $X$ (or $Y$) is produced and released; the receiver module where $Y$ (or $X$) is detected; and an inhibitory module which inhibits the transmitter activity in the presence of the receiver complex.

To facilitate the analysis, we separate the transmitter module of $A$ and receiver module of $B$ and merge them into a “transceiver” module for the diffusible species $X$, which also includes the diffusion process (similarly for the transceiver of $Y$). The network is represented in Figure 2. Each compartment is represented with a block labeled $H_A$ or $H_B$, corresponding to the inhibitory circuit of types $A$ and $B$, respectively. The concentration of the autoinducer synthase for the production of $X$ (respectively, $Y$) is denoted by $y_A$ ($y_B$), and $R_A$ ($R_B$) is the concentration of the receiver complex, the result of $Y$ ($X$) binding to the receiver protein.

The transceiver blocks incorporate diffusion in an ordinary differential equation model that describes the concentrations of the diffusible species in each compartment. We define an undirected graph $\mathcal{G} = \mathcal{G}(V, E)$ where each element of the set of vertices $V$ represents one compartment, and each edge $(i, j) \in E$ represents a channel between compartments $i$ and $j$. For each edge $(i, j) \in E$ we define a weight $d_{ij} = d_{ji}$. The constant $d_{ij}$ is proportional to the

diffusivity of the species and inversely proportional to the square of the distance between compartments. We define the weighted Laplacian:

$$\{L\}_{ij}=\begin{cases} -\sum_{j=1}^{N} d_{ij} & \text{if } i=j \\ d_{ij} & \text{if } i \neq j. \end{cases} \quad (1)$$

The dynamical model of the transceiver tx/rx for *X* is then:

$$\text{tx/rx}_{A\to B}: \begin{cases} \begin{bmatrix} \dot{X}_A \\ \dot{X}_B \end{bmatrix} = \begin{bmatrix} \Gamma_X(X_A, y_A) \\ \Phi_X(X_B, R_B) \end{bmatrix} + L \begin{bmatrix} X_A \\ X_B \end{bmatrix} \\ \dot{R}_B = \Psi_X(X_B, R_B), \end{cases} \quad (2)$$

where $X_A \in \mathbb{R}_{\geq 0}^{N_A}$ is the concentration of species *X* in compartments *A* due to production, $X_B \in \mathbb{R}_{\geq 0}^{N_B}$ the concentration of species *X* in compartment *B* due to diffusion, and $R_B \in \mathbb{R}_{\geq 0}^{N_B}$ the concentration of complexes in compartment *B* formed by the binding of *X* with a receiver protein. The functions $\Gamma_X(\cdot,\cdot) \in \mathbb{R}_{\geq 0}^{N_A}$, $\Phi_X(\cdot,\cdot) \in \mathbb{R}_{\geq 0}^{N_B}$, and $\Psi_X(\cdot,\cdot) \in \mathbb{R}_{\geq 0}^{N_B}$ are concatenations of the decoupled elements $\gamma_X^i(X_A^i, u^i) \in \mathbb{R}_{\geq 0}$, $i = 1, \ldots, N_A$, $\phi_X^j(X_B^j, R_B^j) \in \mathbb{R}_{\geq 0}$ and $\psi_X^j(X_B^j, R_B^j) \in \mathbb{R}_{\geq 0}$, $j = 1, \ldots, N_B$, and assumed to be continuously differentiable. The function $\gamma_X^i(\cdot,\cdot)$ models the production and the degradation of *X* in compartment *i* of type *A*, the function $\phi_X^j(\cdot,\cdot)$ models the degradation of *X* and the binding of *X* with the receiver protein in compartment *j* of type *B*, and $\psi_X^j(\cdot,\cdot)$ models the binding of the receiver complex in compartment *j* of type *B*. The transceiver $\text{tx/rx}_{B\to A}$ for *Y* is defined similarly.

**Assumption 2.1—**For each constant input $y_A^* \in \mathbb{R}_{\geq 0}^{N_A}$ (and $y_B^* \in \mathbb{R}_{\geq 0}^{N_B}$), the subsystem (2) has a globally asymptotically stable steady-state ( $X_A^*, X_B^*, R_B^*$), which is a hyperbolic equilibrium, *i.e.*, the Jacobian has no eigenvalues on the imaginary axis. Furthermore, there exist positive and increasing functions $T_{AB}^{\text{tx/rx}}: \mathbb{R}_{\geq 0}^{N_A} \to \mathbb{R}_{\geq 0}^{N_B}$ and $T_{BA}^{\text{tx/rx}}: \mathbb{R}_{\geq 0}^{N_B} \to \mathbb{R}_{\geq 0}^{N_A}$ s.t.

$$R_B^* \triangleq T_{AB}^{\text{tx/rx}}(y_A^*), \quad \text{and} \quad R_A^* \triangleq T_{BA}^{\text{tx/rx}}(y_B^*). \quad (3)$$

The increasing property of these maps means that a higher autoinducer synthase input leads to more production and, thus more detection on the receiver side.

Next, we represent the blocks $H_k^i$, $i = 1, \ldots, N$ of type $k \in \{A, B\}$ with models of the form:

$$H_k^i: \begin{cases} \dot{x}_i = f_k(x_i, u_i) \\ y_i = h_k(x_i), \end{cases} \quad (4)$$

where $x_i \in \mathbb{R}_{\geq 0}^n$ describes the vector of reactant concentrations in compartment *i*, $u_i \in \mathbb{R}_{\geq 0}$ the input of *i* (concentration of the receiver complex), and $y_i \in \mathbb{R}_{\geq 0}$ the output of *i*

(concentration of an autoinducer synthase). We denote

$x_k=[x_1^T,\ldots,x_{N_k}^T]^T \in R_{\geq 0}^{nN_k}$, $u_k=[u_1,\ldots,u_{N_k}]^T \in \mathbb{R}_{\geq 0}^{N_k}$, and $y_k=[y_1,\ldots,y_{N_k}]^T \in \mathbb{R}_{\geq 0}^{N_k}$, for $k \in \{A, B\}$.

We assume that $f_k(\cdot,\cdot)$ and $h_k(\cdot)$ are continuously differentiable and further satisfy the following properties:

**Assumption 2.2—**For $k \in \{A, B\}$ and each constant input $u^* \in \mathbb{R}_{\geq 0}$, the subsystem (4) has a globally asymptotically stable steady-state $x^* \triangleq S_k(u^*)$, which is a hyperbolic equilibrium. Furthermore, the maps $S_k:\mathbb{R}_{\geq 0} \to \mathbb{R}_{\geq 0}^n$ and $T_k:\mathbb{R}_{\geq 0}^n \to \mathbb{R}_{\geq 0}$, defined as:

$$T_k(\cdot) \triangleq h_k(S_k(\cdot)), \quad (5)$$

are continuously differentiable, and $T_k(\cdot)$ is a positive, bounded and decreasing function.

The decreasing property of $T_k(\cdot)$ is consistent with lateral inhibition, since higher input in one cell leads to lower output.

## B. When do Contrasting Patterns Emerge?

We now present a method to find steady-state patterns for the system in (2)–(4). Given Assumptions 2.1 and 2.2, the existence of variables $z_A \in \mathbb{R}_{\geq 0}^{N_A}$ and $z_B \in \mathbb{R}_{\geq 0}^{N_B}$ such that:

$$\begin{cases} z_A &= \mathbf{T}_A(\mathbf{T}_{BA}^{\mathrm{tx/rx}}(\mathbf{T}_B(\mathbf{T}_{AB}^{\mathrm{tx/rx}}(z_A)))) \\ z_B &= \mathbf{T}_B(\mathbf{T}_{AB}^{\mathrm{tx/rx}}(\mathbf{T}_A(\mathbf{T}_{BA}^{\mathrm{tx/rx}}(z_B)))) \end{cases} \quad (6)$$

with $\mathbf{T}_A(u_A)=[T_A(u_A^1),\ldots,T_A(u_A^{N_A})]^T:\mathbb{R}_{\geq 0}^{N_A} \to \mathbb{R}_{\geq 0}^{N_A}$ (similar for $\mathbf{T}_B(u_B):\mathbb{R}_{\geq 0}^{N_B} \to \mathbb{R}_{\geq 0}^{N_B}$), is sufficient to conclude the existence of a steady-state for the full system (2)–(4). Our goal is to determine when $z_A$ and $z_B$ exhibit contrasting values.

We use the notion of *equitable partition* [8] to reduce the dimension of the maps in (6). For a weighted and undirected graph $\mathcal{G}(V, E)$, with Laplacian matrix $L$, a partition of the vertex set $V$ into classes $O_1, \ldots, O_r$ is said to be *equitable* if there exists $d_{ij}$ for $i, j = 1, \ldots, r$, such that

$$\sum_{v \in O_j} d_{uv} = \bar{d}_{ij} \quad \forall u \in O_i,\ i \neq j. \quad (7)$$

This means that the sum of the edge weights from a vertex in a class $O_i$ into all the vertices in a class $O_j$ ($i \neq j$) is invariant of the choice of the vertex in class $O_i$. We let the *quotient Laplacian* $\bar{L} \in \mathbb{R}^{r \times r}$ be formed by the off-diagonal entries $\bar{d}_{ij}$, and $\{\bar{L}\}_{ii}=\{L\}_{ii}=-\sum_{j=1,j\neq i}^{r}\bar{d}_{ij}$.

**Assumption 2.3—**The partition of the compartments $V$ into the classes $O_A$ of type $A$ and $O_B$ of type $B$ is equitable.

This implies that the total incoming edge weight of the species $X$ (and $Y$) is the same for all the compartments of type $B$ ($A$). For example, the network in Figure 1(left) is equitable with respect to the classes $O_A$ and $O_B$ if $d_{13} + d_{14} = d_{23} + d_{24}$ and $d_{13} + d_{23} = d_{14} + d_{24}$. Since the edge weights $d_{ij}$ are inversely proportional to the square of the distance, this means that opposite channels must have the same length, thus exhibiting a parallelogram geometry.

Assumption 2.3 allows us to search for solutions to (6) where the compartments of the same type have the same steady-state, *i.e.*,

$$z=[\overline{z}_A,\ldots,\overline{z}_A,\overline{z}_B,\ldots,\overline{z}_B]^T=[\overline{z}_A\mathbf{1}_{N_A}^T,\overline{z}_B\mathbf{1}_{N_B}^T]^T \quad (8)$$

where $z_A^- \in \mathbb{R}_{\geq 0}$ and $z_B^- \in \mathbb{R}_{\geq 0}$. This means that the transceiver input-output maps become decoupled and $T_{AB}^{\mathrm{tx/rx}}(\overline{z}_A\mathbf{1}_{N_A})=T_{AB}(\overline{z}_A)\mathbf{1}_{N_B}$, with $T_{AB}$: $\mathbb{R}_{\geq 0} \to \mathbb{R}_{\geq 0}$. The same holds for $T_{BA}^{\mathrm{tx/rx}}(\cdot)$ with $T_{BA}$: $\mathbb{R}_{\geq 0} \to \mathbb{R}_{\geq 0}$. Furthermore, $z_A^-$ and $z_B^-$ satisfy the following reduced system of equations:

$$\begin{cases} \overline{z}_A &= T_A(T_{BA}(T_B(T_{AB}(\overline{z}_A)))) \triangleq \overline{T}_A(\overline{z}_A) \\ \overline{z}_B &= T_B(T_{AB}(T_A(T_{BA}(\overline{z}_B)))) \triangleq \overline{T}_B(\overline{z}_B) \end{cases}, \quad (9)$$

where $T_A^-$: $\mathbb{R}_{\geq 0} \to \mathbb{R}_{\geq 0}$ and $T_B^-$: $\mathbb{R}_{\geq 0} \to \mathbb{R}_{\geq 0}$ are a composition of scalar maps. Let $z_A^{\sim}$ be a solution to the top equation in (9), then $z_B^{\sim} \triangleq T_B(T_{AB}(z_A^{\sim}))$ must be a solution to the bottom one.

From Assumptions 2.1 and 2.2, $T_A^-(\cdot)$ and $T_B^-(\cdot)$ in (9) are positive, increasing and bounded functions. Figure 3 illustrates typical shapes of the input-output maps $T_A^-(\cdot)$ and $T_B^-(\cdot)$. In Fig. 3(a) there exists only one solution (orange circles). This is a *near-homogeneous* steady-state, where the discrepancy between $z_A^{\sim}$ and $z_B^{\sim}$ is due only to nonidentical $T_A^-(\cdot)$ and $T_B^-(\cdot)$. The map $T_A^-(\cdot)$ in Fig. 3(b) has three fixed points: a middle solution (near-homogenous steady-state), a large fixed point (blue triangle), and a small fixed point (green square). The latter two have a corresponding opposite fixed point in $T_B^-(\cdot)$, specifically $z_B^{\sim} \triangleq T_B(T_{AB}(z_A^{\sim}))$, and therefore represent a contrasting steady-state pattern.

Note that a contrasting pattern emerges when the near-homogenous steady-state has a slope greater than 1, that is:

$$\left.\frac{d\overline{T}_A}{dz_A}\right|_{z_A} = T'_{AB}(\tilde{z}_A)T'_B(T_{AB}(\tilde{z}_A))\,T'_{BA}(\tilde{z}_B)T'_A(T_{BA}(\tilde{z}_B)) > 1. \quad (10)$$

Indeed, due to the boundedness and strictly increasing properties of the map $T_A^-(\cdot)$, there must exist two other fixed point pairs of (9),$(z_A^*, z_B^* \triangleq T_B(T_{AB}(z_A^*)))$ and $(z_A^{**}, z_B^{**})$ for which

$$(z_A^* > \tilde{z}_A \quad \text{and} \quad z_B^* < \tilde{z}_B) \quad (z_A^{**} < \tilde{z}_A \quad \text{and} \quad z_B^{**} > \tilde{z}_B). \quad (11)$$

We show that (10) implies that the near-homogenous steady-state is unstable, setting the stage for contrasting patterns and providing a parameter tuning principle for patterning.

### C. Convergence to Contrasting Patterns

To analyze convergence to the steady-state patterns in (9), we employ monotonicity assumptions. A *monotone* system is one that preserves a partial ordering of the initial conditions as the solutions evolve in time. A partial ordering is defined with respect to a *positivity cone* in the Euclidean space that is closed, convex, pointed ($K \cap (-K) = \{0\}$), and has nonempty interior. In such a cone, $x \preceq x$ means $x \hat{-} x \in K$. Given the positivity cones $K^U$, $K^Y$, $K^X$ for the input, output, and state space, the system $\dot{x} = f(x, u)$, $y = h(x)$ is said to be *monotone* if $x(0) \preceq x(\hat{0})$ and $u(t) \preceq \hat{u}(t)$ for all $t \geq 0$ imply that the resulting solutions satisfy $x(t) \preceq x(\hat{t})$ $\forall t \geq 0$, and the output map is such that $x \preceq x$ implies $h(x) \preceq h(x)$ [9].

**Assumption 2.4—**The system tx/rx$_{A\to B}$ in (2) is monotone with respect to $K^U = \mathbb{R}_{\geq 0}^{N_A}$, $K^Y = \mathbb{R}_{\geq 0}^{N_B}$, and $K^X = \mathbb{R}_{\geq 0}^{N+N_B}$. Similarly tx/rx$_{B\to A}$ is monotone with respect to $K^U = \mathbb{R}_{\geq 0}^{N_B}$, $K^Y = \mathbb{R}_{\geq 0}^{N_A}$, and $K^X = \mathbb{R}_{\geq 0}^{N+N_A}$.

**Assumption 2.5—**The systems $H_A$ and $H_B$ in (4) are monotone with respect to $K^U = -K^Y = \mathbb{R}_{\geq 0}$, and $K^X = K$, where $K$ is some positivity cone in $\mathbb{R}$.

These monotonicity assumptions are consistent with Assumptions 2.1–2.2, as they imply the increasing property of $T_{BA}^{\text{tx/rx}}(\cdot), T_{AB}^{\text{tx/rx}}(\cdot)$, and the decreasing behavior of $T_A(\cdot)$, $T_B(\cdot)$.

**Theorem 2.6—**Consider the network (2)-(4) and suppose Assumptions 2.1, 2.2, 2.4 and 2.5 hold. Let the partition of the compartments into the classes $O_A$ and $O_B$ be equitable. The steady-state described by (9) is asymptotically stable if

$$T'_{AB}(\tilde{z}_A) T'_B(T_{AB}(\tilde{z}_A)) T'_{BA}(\tilde{z}_B) T'_A(T_{BA}(\tilde{z}_B)) < 1, \quad (12)$$

and unstable if (10) holds.

## III. Example

In this section we study an example in which each block $H_k^i$, $i = 1, \ldots, N$ of type $k \in \{A, B\}$ is represented as

$$H_{A/B}^i : \begin{cases} \dot{x}^i & = v_T \left( \frac{1}{1 + \left( R^i_{A/B} / K_T \right)^{n_T}} + \ell \right) - \gamma_{I_{X/Y}} x^i \\ p^i_{I_{X/Y}} & = c x^i \end{cases} \quad (13)$$

where $n_T$ represents the cooperativity, $\gamma_{I_{X/Y}}$ is the degradation rate, $\ell$ the leakage rate, $K_T$ the dissociation constant, $\nu_T$ the velocity rate, and $c$ is a scaling factor. The variable $x^i \in \mathbb{R}_{\geq 0}$, represents the concentration of a signaling protein (*e.g.*, RFP) in compartment $i$, as well as the output concentration $p^i_{I_{X/Y}} \in \mathbb{R}_{\geq 0}$ of autoinducer synthase.

For the dynamics of the transceiver, we choose two quorum sensing pairs where the binding of the autoinducer synthase to the receptor is orthogonal with respect to autoinducer/receptor pairs. We denote by $X$ and $Y$ the concentration of diffusible molecules and by $R_B$ and $R_A$ the concentration of complexes at colonies of type $B$ and $A$, respectively. For the transceiver of $X$, we consider $X^i_A$, $i = 1, \ldots, N_A$ to be the concentration of species $X$ in compartment $i$ of type $A$, and $X^j_B$, $j = 1, \ldots, N_B$ the concentration of species $X$ in compartment $j$ of type $B$. Let $[X^T, R^T_B]^T$ be the transceiver state, with $X = [X^T_A, X^T_B]^T = [X^1_A, \ldots, X^{N_A}_A, X^1_B, \ldots, X^{N_B}_B]^T$ and $R_B = [R^1_B, \ldots, R^{N_B}_B]^T$. The transceiver dynamics are:

$$\mathrm{tx/rx}_{A\to B}: \begin{cases} \frac{d}{dt}X^i_A &= \nu p^i_{I_X} - \gamma_X X^i_A + L_i X \\ \frac{d}{dt}X^j_B &= -k_{on} X^j_B (p_{R_X} - R^j_B) + k_{off} R^j_B + -\gamma_X X^j_B + L_{j+N_A} X \\ \frac{d}{dt}R^j_B &= k_{on} X^j_B (p_{R_X} - R^j_B) - k_{off} R^j_B, \end{cases} \quad (14)$$

where $L_i$ corresponds to the row $i$ of the Laplacian matrix, $p_{R_k}$ is the constitutive concentration of the receiver protein (bound and unbound), $k_{on}/k_{off}$ are the binding rates, and $\nu$ is the generation rate of the diffusible molecule. The dynamics for the inhibitory circuit of cell type $B$ and for the transceiver $\mathrm{tx/rx}_{B\to A}$ are obtained similarly.

For the analysis, note that $H_A$, $H_B$ and $\mathrm{tx/rx}_{A\to B}$, $\mathrm{tx/rx}_{B\to A}$, meet the assumptions in the previous section.

**Lemma 3.1**

The transceiver dynamics in (14) meet Assumptions 2.1 and 2.4.

Under Assumption 2.3, we analyze the range of parameters where patterning occurs by looking for steady-states that are fixed points of the scalar maps $T_A(\cdot)$ as in (9)[1]. We use reaction parameters that correspond to the values suggested in [10, Parameter Set 1]. The slope of these maps at the fixed points depends on the edge weights $d_{ij}$ and constitutive concentration of total LuxR $p_{Ri}$, which are tunable parameters. We can tune $d_{ij}$ by changing the channel lengths, and $p_{R_i}$ by changing the strength of the constitutive promoter. We consider two compartments connected by one channel, one of type $A$ and the other of type $B$. This is equivalent to considering any equitable network topology with the same $\bar{d}_{AB}$ and $\bar{d}_{BA}$.

[1] with the decoupled transceiver input-output scalar map $T_{AB}(\tilde{z}_A) = \left(1 + \frac{k_{off}}{k_{on}} \frac{\gamma_X(\gamma_X + \bar{d}_{AB} + \bar{d}_{BA})}{\bar{d}_{BA}\nu} \frac{1}{\tilde{z}_A}\right)^{-1}$, where $\bar{d}_{AB}$ and $\bar{d}_{BA}$ as in (7)

Figure 4 maps the regions over the tunable pairs ($p_{R_i}$, $d_{ij}$) where contrasting patterns emerge. At the extreme values, if the concentration of $p_{R_i}$ is too low, the detection ability of each cell is affected, which leads to a low concentration of the receiver complex. Thus, no cell is being inhibited and no contrasting patterning emerges. When $p_{R_i}$ is too high, both compartments are inhibited since both cells are too sensitive to the receiver signal due to leakage.

Further analysis using condition (10) reveals that the circuit, for this set of parameters, is fairly robust to parameter uncertainty. We introduced a variation of 10% in each parameter and the patterning range didn't suffer significant change. Patterning occurs when $n_T \geq 2$, greater $n_T$ implies stronger inhibition and shifts the patterning region slightly to the left.

For validation, we implemented a partial differential equations (PDEs) compartment network, using the finite element solver COMSOL. For shorter channels ($\leq 4mm$), we compute a correction factor for the ODE model, that compensates for the extra degradation of the diffusible molecule along the channels. In these regimes, we obtain an accurate steady-state and dynamical match between the ODE and the PDE model.

When the equitability condition is satisfied approximately rather than exactly, we treat the system as a perturbation of an equitable one and appeal to continuous dependence of solutions on the parameters $d_{ij}$.

## Supplementary Material

Refer to Web version on PubMed Central for supplementary material.

## Acknowledgments

This research was supported by the NIH National Institute of General Medical Sciences, grant 1R01GM109460-01.

## References

1. Meinhardt H, Gierer A. Pattern formation by local self-activation and lateral inhibition. BioEssays. 2000; 22(8):753–760. [PubMed: 10918306]
2. Collier J, Monk N, Maini P, Lewis J. Pattern formation by lateral inhibition with feedback: a mathematical model of Delta-Notch intercellular signalling. J Theoret Biol. 1996; 183(4):429–446. [PubMed: 9015458]
3. Sprinzak D, Lakhanpal A, LeBon L, Garcia-Ojalvo J, Elowitz MB. Mutual inactivation of Notch receptors and ligands facilitates developmental patterning. PLoS Comput Biol. Jun.2011 7
4. Rufino Ferreira A, Arcak M. A graph partitioning approach to predicting patterns in lateral inhibition systems. SIAM Journal on Applied Dynamical Systems. 2013; 12(4):2012–2031.
5. Aoki SK, Diner EJ, de Roodenbeke CT, Burgess BR, Poole SJ, Braaten BA, Jones AM, Webb JS, Hayes CS, Cotter PA, Low DA. A widespread family of polymorphic contactdependent toxin delivery systems in bacteria. Nature. 2010; 468(7322):439–442. [PubMed: 21085179]
6. Collins CH, Leadbetter JR, Arnold FH. Dual selection enhances the signaling specificity of a variant of the quorum-sensing transcriptional activator LuxR. Nat Biotech. 2006; 24(6):708–712.
7. Balagaddé FK, Song H, Ozaki J, Collins CH, Barnet M, Arnold FH, Quake SR, You L. A synthetic Escherichia coli predator–prey ecosystem. Molecular Systems Biology. 2008; 4(1):187. [PubMed: 18414488]
8. Godsil, C.; Royle, G. Algebraic Graph Theory. Springer; Apr. 2001

9. Angeli D, Sontag E. Monotone control systems. IEEE Trans Automat Control. Oct.2003 48:1684–1698.

10. Hsia J, Holtz WJ, Huang DC, Arcak M, Maharbiz MM. A feedback quenched oscillator produces Turing patterning with one diffuser. PLoS Comput Biol. Jan.2012 8:e1002331. [PubMed: 22291582]

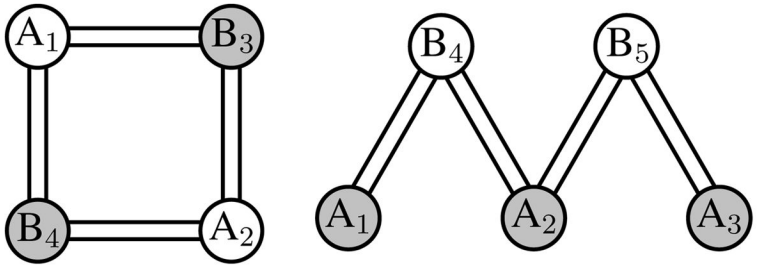


**Figure 1.**

Compartmental lateral inhibition system with cells of type *A* and *B*, where contrasting patterns between neighboring compartments emerge. In each compartment $A_i$ ($B_i$) we place a colony with cells of type *A* (*B*) that communicate through channels. Each cell type can only detect signaling molecules produced by the other type, preventing auto-inhibition.

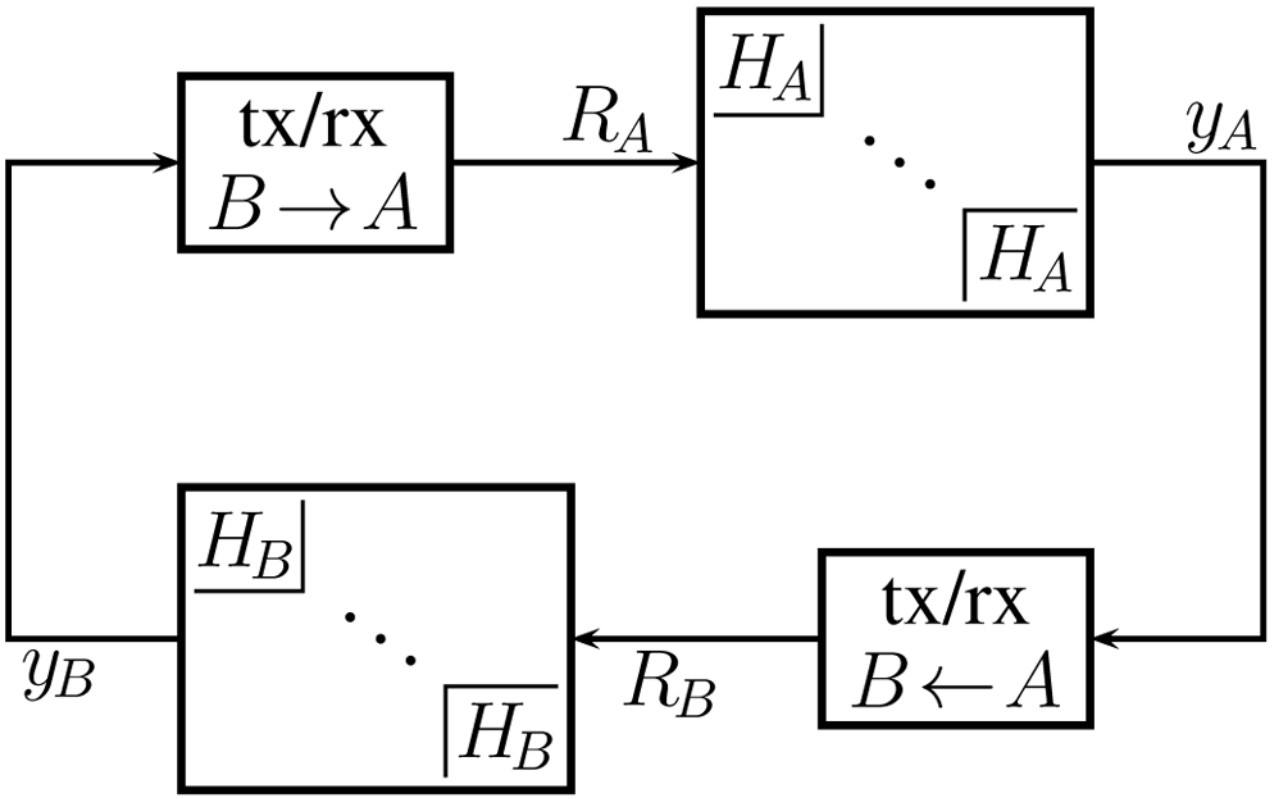


**Figure 2.**

Block diagram for two types of compartments *A* and *B* communicating through diffusion. For each type of diffusible species, the transceiver includes the dynamics of the senders' transmitter modules, the receivers' detection modules, and the diffusion process.

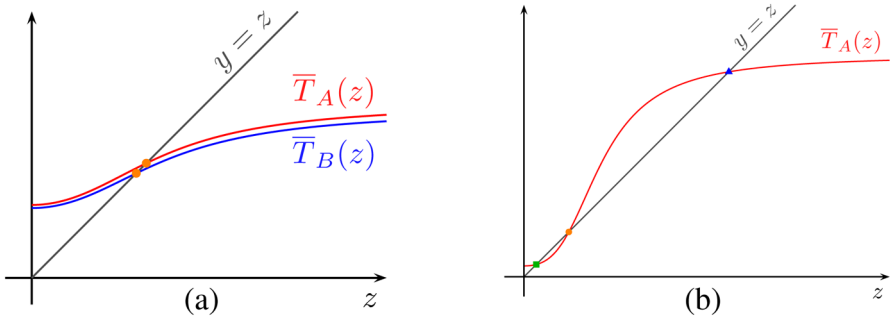


**Figure 3.**

Typical shapes of input-output maps $\bar{T}_A(\cdot)$ and $\bar{T}_B(\cdot)$: (a) The unique pair of fixed points (orange circles) is near-homogenous and no contrasting patterns emerge; (b) There exist three pairs of fixed points (orange circle, green square, and blue triangle), and the two additional solutions represent contrasting steady-state patterns.

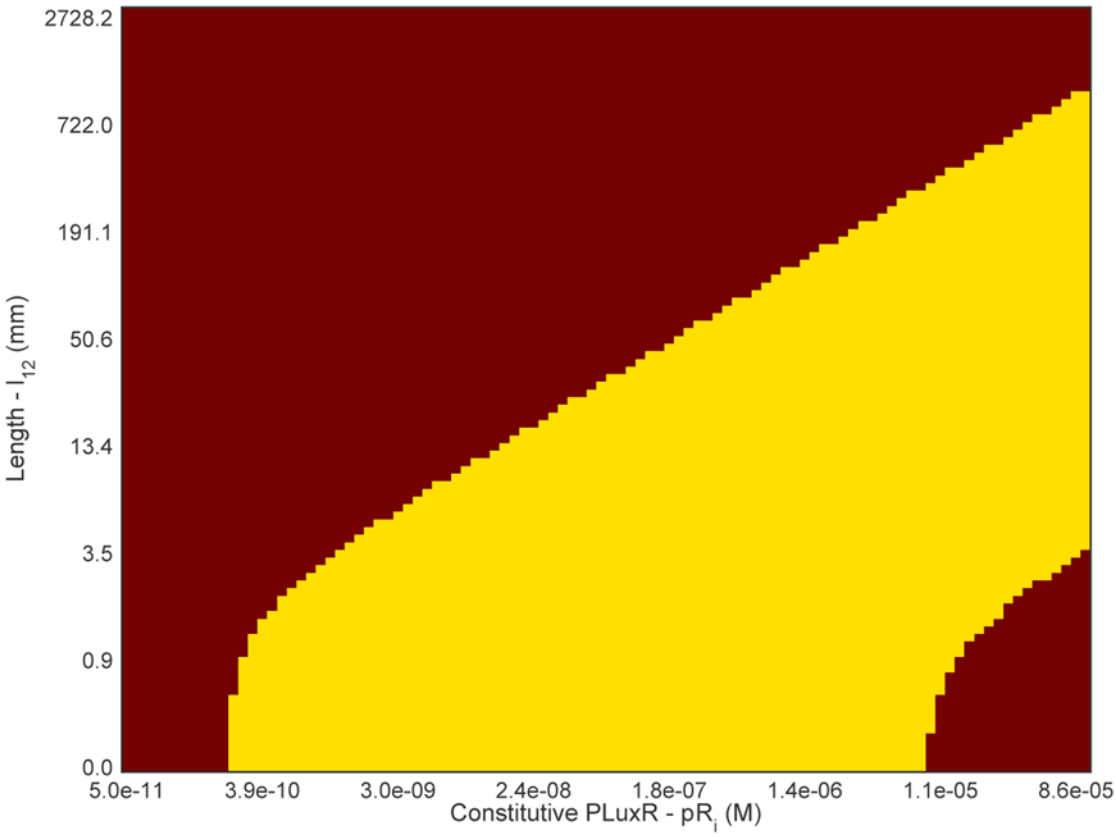


**Figure 4.**

Patterning (yellow) vs. non-patterning (red) region, for varying $p_{R_i}$ and $d_{AB}^{-} = d_{BA}^{-}$, and where: $n_T = 2$; $c = 1$; $\nu = 1.34e\text{-}2s^{-1}$; $\gamma_X = 7.7e\text{-}4s^{-1}$; $k_{on} = 1e9s^{-1}M^{-1}$; $k_{off} = 50s^{-1}$; $v_T = 1.03e\text{-}11s^{-1}M$; $K_T = 2.68e19M$; $\ell = 1.98e\text{-}4$; $\gamma_{I_X} = 1.16e\text{-}3s^{-1}$.